DOI: 10.1002/ ((please add manuscript number))

Article type: Full Paper

Synergistic interaction of Dyes and Semiconductor Quantum Dots for Advanced Cascade Co-Sensitized Solar Cells

*Vicente M. Blas-Ferrando, Javier Ortiz, Victoria González-Pedro, Rafael S. Sánchez, Iván Mora-Seró, Fernando Fernández-Lázaro and Ángela Sastre-Santos**

V. M. Blas-Ferrando, Dr. J. Ortiz, Prof. F. Fernández-Lázaro and Prof. Á. Sastre-Santos
División de Química Orgánica Instituto de Bioingeniería, Universidad Miguel Hernández, Elche 03202, Spain.
E-mail: asastre@umh.es

Dr. V. González-Pedro, Dr. R. S. Sánchez and Prof. I. Mora-Seró
Grup de Dispositius Fotovoltaics i Optoelectrònics, Departament de Física, Universitat Jaume I, 12071 Castelló, Spain
E-mail: sero@uji.es

Keywords: phthalocyanine, quantum dots, Grätzel solar cells

Abstract.

Here, we report a new procedure for the co-sensitization with quantum dots (QDs) and dyes for sensitized solar cell. Cascade co-sensitization of TiO_2 electrodes are obtained by the sensitization with CdS quantum dots (QDs) and zinc phthalocyanines (ZnPcs), in which ZnPcs containing sulfur atom have been specially designed to produce a cascade injection by attaching directly to QDs. This strategy causes a double synergetic interaction. This is the differentiating point of cascade co-sensitization in comparison with other approach in which dyes with conventional functionalization are employed, that pursue anchoring dyes to TiO_2

electrodes. Co-sensitization produces a panchromatic response from the visible to near IR region already observed with other sensitization strategies. However, cascade co-sensitization produces in addition a synergistic interaction between QDs and dye, that it is not merely limited to the complementary light absorption, but dye enhances the efficiency of QD sensitization acting as a passivating agent. Cascade Co-sensitization concept has been demonstrated with using /[Co(phen)$_3$]$^{3+/2+}$ redox. The TiO$_2$/CdS QD-ZnPc/[Co(phen)$_3$]$^{3+/2+}$ sensitized solar cell shows a big improvement of short circuit photocurrent and open-circuit voltage in comparison with samples simply sensitized with QDs. The advent of such co-sensitized QD-ZnPc sensitized solar cells paves the way to extend the absorbance region of the promising QD-based solar cells and the development of a new family of molecules designed for this purpose.

1. Introduction

An elegant strategy to improve the light-harvesting in photovoltaic devices is to use complementary light harvesters capable to produce panchromatic absorption. Here we have combined semiconductor quantum dots (QDs) and *ad hoc* designed phthalocyanines (Pcs) in order to prepare sensitized solar cells with enhanced efficiency. QDs are among potential key players in the next generation of photovoltaic devices [1] due to their low-cost solution-phase processability, large absorption cross sections, a spectrally tunable absorption onset (achieved via the quantum size effect), and enhanced multiple exciton generation or carrier multiplication.[2] After the first report on a certified QD solar cell,[3] a remarkable progress has been reached just in a couple of years obtaining certified power conversion efficiencies (PCEs) approaching 9%.[4]

On the other hand, Pcs are outstanding dye candidates in dye sensitized solar cells (DSSCs) due to their high extinction coefficient in the infrared spectral region and to their high thermal and chemical stabilities.[5] Pcs incorporated in DSSCs have achieved PCEs as high as 6.4 %,[6] still far away from the 12.75% PCE obtained by porphyrins,[7] their closest relatives. Light harvesting ability of QDs and Pcs can be enhanced by binding them, either covalent or supramolecular, producing a system capable to charge injection from both chromophores. However, the chemical combination of Pc rings to QDs has hardly been explored probably due to the difficulties to synthesize Pcs with the adequate anchoring groups. Until now just a few articles have been published where Pcs are covalently linked to QDs showing in most of the cases Förster resonance energy transfer (FRET) from QDs to Pcs. SiPc has been connected to CdSe QDs through axial ligation,[8] and also tetraminoZnPc[9] and unsymmetrically tris-*tert*-butyl-imidoZnPc[10] have been linked to CdSe showing FRET and quenching the QDs emission. But few complete photovoltaic devices taking benefit of this interaction are reported. Nazeeruddin, Grätzel *et col* published a very interesting seminal work on co-sensitization where zinc carboxyphthalocyanine dye (TT1) is added on top of a TiO_2/PbS-sensitized electrode, prepared by successive ionic layer absorption and reaction (SILAR), to obtain a panchromatic response, which results in an improved efficiency *versus* the TiO_2/TT1 system.[11] TT1 dye as most of the dyes was designed with a carboxylic group to attach to TiO_2. These authors obtained co-sensitized cells with enhanced efficiency due to the broadening of the light absorption region. Another examples of co-sensitization of this kind have been reported with CdS and SQ1.[11] Nevertheless a close inspection of the external quantum efficiency (EQE) showed a decrease of the performance in the light absorption region of QDs after co-sensitization. Conversely very recently, we have shown that it is possible to enhance the performance in the light absorption region of QDs with an appropriated QD passivation. Disulphide bisphthalocyanine was covalently bonded to CdSe and CdS QDs improving, by a passivation mechanism, the efficiency of the QD solar cell compared with the QD without phthalocyanine.[12] In our previous work, despites the improvement in cell efficiency with the co-sensitization, no contribution from the ZnPc in the EQE was observed probably due to the non-conjugated bridge between the sulphur anchoring group and the ZnPc. Here, we show that cascade co-sensitization by the use of especially designed ZnPc that can produce both beneficial effects, broadening of light absorption and QD passivation.

Here we will like to highlight the synthesis of phthalocyanines designed for anchoring selectively on semiconductor QDs in TiO_2/QDs electrodes by a thiol (SH) group. These two new mercaptophthalocyanines dyes, where SH is either directly connected to the macrocycle or through a conjugated linker, exhibit the capability of injecting electrons into the QD. Therefore, we have proved in this work a cascade injection from the ZnPcs into the TiO_2 electrode though the CdS QD, with contributions of both sensitizers to the EQE. In addition, ZnPc passivates the surface of QDs enhancing the EQE of the QD-sensitizer in comparison with devices prepared without co-sensitization. Several trials to synthesize thiol substituted phthalocyanines were unsuccessful in our hands, mostly attributable to the SH oxidation catalysed by the own phthalocyanine ring.[13] For this reason, we have synthetized two unsymmetrically substituted phthalocyanines, **CNC_2H_4SZnPc 1** and **$AcSPhC_2ZnPc$ 2** (Scheme 1 and 2), with different protecting groups in the sulphur, ethylennitrile and thioester, respectively, to avoid oxidation. Moreover, these Pcs present donor substituents, such as *tert*-octylphenoxy and *tert*-butyl groups, to increase the energy of the LUMO levels over the conduction band of the CdS QD in order to facilitate the electron injection, and place the HOMO levels lower in energy than the electrolyte for efficient charge regeneration (Figure 1).

2. Results and Discussion

CNC_2H_4SZnPc **1** was prepared by statistical condensation of 4-(2-cyanoethyl)thiophthalonitrile (**3**) and bis(*p-tert*-octylphenoxy)phthalonitrile[14] to get the free base $CNC_2H_4SH_2Pc$ **4** followed by zinc metalation (Scheme 1). $AcSPhC_2ZnPc$ **2** was achieved by Sonogashira coupling of iodotri-*tert*-butylphthalocyaninate zinc (II)[15] with 4-ethynyl-1-acetylthiobenzene[16] in a pretty good yield (Scheme 2). For electrode sensitization, first CdS QDs are directly deposited on mesoporous TiO_2 substrate by SILAR method (see experimental section for further details). Prior to the co-sensitization of the SILAR prepared TiO_2/CdS sensitized electrodes, the elimination reaction of the protecting groups of ZnPCs has been carried out by reaction with CsOH, thus allowing obtaining CdS QD-SZnPc and CdS QD-$SPhC_2ZnPc$ hybrid systems (Scheme 3).

UV-vis spectra in THF as solvent show typical Q and B Pc absorption bands with high extinction coefficients corresponding to non-aggregated Pcs centered respectively at 682 and 361 nm for CNC_2H_4SZnPc and 686, 671 (Q band splitting due probably to the presence of 4 different regioisomers) and 351 nm for $AcSPhC_2ZnPc$ (Figure 2a). Figure 2b confirms by UV-vis in solid state of the QDSC devices that the two Pcs have been attached to the CdS-QD, observing the Q bands of the ZnPcs at the same wavelength that in THF solution. However, the UV-vis band of QD in the hybrid CdS-ZnPcs increased in intensity and appears at 475 nm, 28 nm batochromically shiftted compared with the pristine QD band centered at 447 nm. This fact could be explained by the reduction of quantum confinement after being covered by the big macrocyclic ring. Moreover, comparing the Q-band intensity of the two ZnPcs, a larger amount of load is observed for CNC_2H_4SZnPc than for $AcSPhC_2ZnPc$. This factor is also observable by the naked eye comparing the green colour intensity of the devices (Figure 2c).

Figure 3a shows the current-potential (J-V) curves comparing the Pc-untreated CdS device as a reference, with our CdS-SZnPc hybrid systems using S^{2-}/S_n^{2-} as electrolyte. Higher open-circuit voltage (V_{oc}) and short circuit current (J_{sc}) were obtained when ZnPcs were attached to the CdS QD (Table 1). It is very important to note that the new ZnPcs dyes here reported do not attach directly to TiO_2 as we have verified experimentally. Figure 3b shows the EQE *versus* wavelength for these cells. A significant increase of the EQE in the area between 300 and 500 nm is observed, however, it does not occurs the same in the area of 600-700 nm where the phthalocyanine absorbs, concluding that the main effect of QD-dye interaction is the passivation of the QD surface,[12, 17] but no evidence of cascade injection from dye into TiO_2 electrode, through the QD is observed. The introduction of the Pc dyes increases the efficiency around 50%, from 1.1 % up to 1.7 % in CdS QD-SZnPc and 1.5 % in CdS QD-$SPhC_2ZnPc$ 2 (Table 1).

However, these results were significantly improved by changing the electrolyte to $[Co(phen)_3]^{3+/2+}$. Thus, the devices CdS QD:ZnPcs showed a big increase in both the short circuit current and the open-circuit voltage going from 2.49 $mA\cdot cm^{-2}$/654 mV in the CdS used as reference to 6.02 $mA\cdot cm^{-2}$/750 mV in CdS QD-SZnPc and 4.52 mA/cm^2/734 mV in CdS QD-$SPhC_2ZnPc$ (Figure 4a). These enhancements for the co-sensitized systems are understandable paying attention to the EQE spectra (Figure 4b); the contribution of the ZnPcs within the 600-800 nm region can be observed in addition to the contribution of QDs in the 300-500 nm region. Furthermore, an increase of FF is also reported for co-sensitized samples, see (Table 1). As a result, the overall performance of the co-sensitized device is increased from 0.8% using CdS QD as sensitizers to 2.5 % and 1.9 % with co-sensitization for CdS QD-SZnPc and CdS QD-$SPhC_2ZnP$, respectively. This increase represents a three-fold and two-fold enhancement, respectively, in the power conversion efficiency. From the J-V curve and

EQE spectra, we can infer that the TiO_2/CdS-ZnPc/$[Co(phen)_3]^{3+/2+}$ solar cell device delivers a photovoltaic response from both materials. In addition, resonant Förster energy transfer can be rule out due to the low overlaping between dye emission and QD absorption. The enhanced device efficiencies are attributed to the charge injection occurring from both sensitizers, with electron transfer from high energy ZnPc to the lower energy CdS QDs and from QD into TiO_2 demonstrating a cascade co-sensitization. The use of a cobalt electrolyte, with a redox potential closer in energy to the HOMO of the ZnPcs compared to the polysulfide, seems to be a crucial parameter for the regeneration of the dye.

Despite it has been experimentally verified that TiO_2 was not able to be sensitized using ZnPcs **1** and **2**, due to the presence of an inadequate anchoring group, a small contribution from direct injection from ZnPc to the TiO_2 cannot be ruled out. The energetic diagram provided in Figure 1 indicates that the direct electron transfer from dye to TiO_2 is energetically possible. Since QD sensitization is conducted using the SILAR method, leading to a large particle distribution of QDs, it is possible that dye molecules coordinated with small QD particles could bein contact with TiO_2, thus allowing the electron transfer. For this reason, the electron transfer mechanism will be analysed using femtosecond transient flash photolysis measurements and the conclusions will be published elsewhere.

To unveil the origin of this enhanced performance cells plotted in Figure 4a-b have been characterized by impedance spectroscopy and analysed with the standard models for QDSCs.[18, 19] The compared values obtained for recombination resistance, R_{rec}, and chemical capacitance, C_μ, are depicted in Figure 5(a) and (b), respectively. The similar values obtained for both magnitudes, see (Figure 5), independently of the dye used indicate: i) TiO_2 conduction band does not change depending on the employed dye, because the same C_μ is observed; ii) Recombination rate does not vary, as the same R_{rec} has been obtained for both systems. Consequently, both solar cells are similar in terms of IS characterization, although their photovoltaic behaviour is clearly different, particularly in terms of J_{sc} and V_{oc}. The origin of the different photocurrents relies on a process which is not accessible by IS. The higher photovoltaic values obtained for CdS QD-SZnPc *versus* the CdS QD-SPhC$_2$ZnPc device can be explained by the closer distance between both QD and ZnPc in the first case that could make the electron transfer more favorable and/or by the higher dye loading. Higher dye loading with SZnPc is confirmed by taking into account the extinction coeficeint, Figure 2(a) and the absorption measurements Figure 2(b). Different injection rate could also contribute to this effect but this point is beyond the scope of the present communication.

3. Conclusion

This work reports, for the first time, on the cascade co-sensitization using QD and dyes. We have demonstrated this concept with CdS QDs and *ad hoc* designed ZnPcs with thiol groups in a sensitized solar cell where the dye is selectively anchored to the QDs. As a result of this co-sensitization, the photocurrent, open circuit voltage and FF are increased. Efficiency of co-sensitized CdS QD-SZnPc, with Co(phen)$_3$]$^{3+}$/[Co(phen)$_3$]$^{2+}$ electrolyte, is 212% higher than cell produced just with CdS QD sensitization. The cascade co-sensitization opens the possibility to achieve devices with a high response in the visible region due to the outstanding QDs properties and to extend their functionality to the NIR by the contribution of ZnPcs. This works stablishes the potentiality of a new family of dyes especially designed for anchoring to QDs instead to high band-gap material, *i.e.* TiO$_2$. The fact that individual QDs already demonstrated high efficiency opens up new avenues for future improving these efficiencies by co-sensitization with properly designed dyes. Cascade co-sensitization allows a synergistic panchromatic light absorption, on one side, with recombination reduction by means of surface passivation in the presence of an appropriate electrolyte, on the other side. This work could have important implications on the future development of sensitized devices.

4. Experimental Section

Materials and methods for the synthesis of new compounds. All chemicals were reagent-grade, purchased from commercial sources, and used as received. Column chromatography was performed using SiO_2 (40-63μm) TLC plates coated with SiO_2 60F254 and visualized by UV light. NMR spectra were measured with a Bruker AC 300. Fluorescence spectra were recorded with Perkin-Elmer LS 55 Luminescence Spectrometer, UV/Vis spectra were recorded with a Helios Gamma spectrophotometer and IR spectra with Nicolet Impact 400D Spectrometer. Mass spectra were obtained from Bruker Microflex matrix-assisted laser desorption/ionization time of flight (MALDI-TOF). CV measurements were performed in a conventional three-electrode cell using a μ-AUTOLAB type III potentiostat/galvanostat at 298 K, over benzonitrile and deaerated sample solutions (~0.5 mM), containing 0.10 M tetrabutylammonium hexafluorophosphate ($TBAPF_6$) as supporting electrolyte. A glassy carbon (GC) working electrode, $Ag/AgNO_3$ reference electrode and a platinum wire counter electrode were employed. Ferrocene/ferrocenium was used as an internal standard for all measurements. Impedance spectroscopy measurements were carried out under dark conditions at different forward biases, by applying a 20mV AC sinusoidal signal over the constant applied bias with the frequency ranging between 400 kHz and 0.1 Hz.

Preparation on Sensitized TiO_2. The electrode configuration was a 9 nm-thicked transparent layer DSL 18NR-T (20 nm average particle size) and a 6 nm-thicked scattering layer WERO-

4 (300-400 nm particle size distribution). The FTO (SnO_2:F) coated glass was previously covered by a compact layer of TiO_2 deposited by spray pyrolysis of titanium(IV)bis(acetoacetonato) di(isopropanoxylate). These electrodes were sintered at 450 °C for 30 min.

The mesoporous TiO_2 electrodes were *in situ* sensitized with CdS QDs grown by SILAR. For CdS growth the electrodes were successively immersed in two different solutions for 1 min each: one consisting of 0.05 M $Cd(OAc)_2$ dissolved in ethanol, another of 0.05 M Na_2S in methanol/Milli-Q ultrapure (1:1). Following each immersion, rinsing and drying was undertaken using a solution without the precursor in order to rinse the excess of precursor. All these processes constitute one SILAR cycle. The SILAR process was carried out using SILAR equipment from ISTest at room temperature under an air atmosphere. All the samples analyzed in this study were coated with five SILAR cycles

General procedure for anchoring ZnPcs to QD. 0.002 mmol of the ZnPc and 0.006 mmol of CsOH were diluted in 500 µl of dried THF in argon atmosphere at room temperature and stirring during 2 h to eliminate the protecting group. After that time, an additional quantity of dried THF was added to obtain 5 mM ZnPc solution. In inert conditions, the mesoporous TiO_2 electrodes sensitized by CdS QDs grown by SILAR were immersed in the 5 mM ZnPc solution for 4 h. Then, the device was washed with dried THF to remove the unattached Zn to the QD.

Solar Cell Configuration. The device preparation was carried out by sandwiching the working electrode (sensitized photoanode) with the Cu_2S or platinized counter electrodes and using the polysulfide or $[Co(phen)_3]^{3+}/[Co(phen)_3]^{2+}$ electrolyte. The Cu_2S counter electrodes were prepared by immersing brass in HCl solution at 70 ºC for 5 min and subsequently dipping into polysulfide solution for 1 min, resulting in a porous Cu_2S electrode. The platinized counter electrode was made applying a drop of 5 mM H_2PtCl_6 in dry 2-propanol and spreading onto the conducting glass substrate (FTO). The coated glass was heated under airflow at 390 ºC for 15 minutes.

The polysulfide electrolyte was 1 M Na_2S, 1 M S, and 0.1 M NaOH solution in Milli-Q ultrapure water. And the $Co^{3+/2+}$ electrolyte was elaborated using $[Co(phen)_3]^{3+}(PF_6^-)_3/[Co(phen)_3]^{2+}(PF_6^-)_2$ complex (0.75 M/0.075 M) and 0.2 M of lithium perchlorate ($LiClO_4$) in a mixture of acetonitrile and ethylene carbonate (4:6/v:v).

Electrode and Cell Characterization. The *J-V* curves were performed using a solar simulator at AM 1.5 G, where the light intensity was adjusted with an NREL-calibrated Si solar cell to 1 sun intensity (100 mW cm^{-2}). The IPCE measurements were performed employing a 150 W Xe lamp coupled with a monochromator controlled by a computer; the photocurrent was measured using an optical power meter 70310 from Oriel Instruments, using a Si photodiode to calibrate the system. The absorption spectra were registered using an AndoriDus DV-420A intensified CCD with thermoelectric cooling coupled with a Newport 77400 MS125 TM spectrograph. Light absorption of electrodes sensitized with CdS was carried out on electrodes without TiO_2 scattering layer. A non-sensitized electrode of TiO_2 prepared in the same way has used as reference sample. The absorption from reference samples has been subtracted in the absorption measurements.

Synthesis of 4-(2-cyanoethyl)thiophthalonitrile (**3**): 1.91 g (21.1 mmol) of 3-mercaptopropanenitrile and 1.11 g (7.02 mmol) of 4-nitrophthalonitrile were dissolved in 22 ml of dried DMF in argon atmosphere during 72 h at room temperature. The reaction crude was diluted in DCM and washed with HCl_{aq}, $NaHCO_3$ and H_2O. The organic layer was dried with $MgSO_4$ and concentrated in vacuum. The compound was purified by column chromatography ($CHCl_3$:Hx/7:3), affording 705 mg (47 %) of a white solid (**1**). m. p.: 155.6°C. ^{1}H-NMR (300 MHz, DMSO-*d*$_6$, δ): 8.12 (d, J_m= 2, 1H, ArH), 7.98 (d, J_o= 8.3, 1H, ArH), 7.83 (dd, J_o= 8.3, J_m=2, 2H, ArH), 3.47 (t, *J*= 6.8, 2H, CH_2S), 2.92 (t, *J*= 6.8, 2H, CH_2CN). ^{13}C-NMR (DMSO-*d*$_6$, δ): 144.3, 133.6, 131.1, 130.7, 118.6, 115.7, 115.3, 115.2, 110.4, 26.3, 17.1. IR (KBr): ν= 3098, 3026, 2237, 1585, 1545, 1487, 1391, 1336, 1198, 1074, 848, 528, 504 cm^{-1}.

Synthesis of 2,3,9,10,16,17-hexakis-[4-(*tert*-octyl)phenoxy]-23-(2-cyanoethyl)thio-phthalocyanine ($CNC_2H_4SH_2Pc$ **4**): 100 mg (0.47 mmol) of 4-(2-cyanoethyl)thiophthalonitrile (**1**) and 755 mg (1.41 mmol) of 4,5-bis(*p*-tert-octylphenoxy)phthalonitrile were dissolved in 1.2 ml of DMAE in argon atmosphere and refluxed for 14 h. Then, the mixture was cooled to room temperature and precipitated adding methanol. The crude was purified by column chromatography using $CHCl_3$:Hx/75:25, yielding 24 mg (3%) of a green powder (**2**). ^{1}H-NMR (300 MHz, $CDCl_3$, δ): 9.08-8.51 (m, 8H, ArH), 7.99 (m, 1H, ArH), 7.61-7.40 (m, 12H, ArH), 7.30-7.13 (m, 12H, ArH), 3.5 (t, *J* = 7.2 Hz, 2H, CH_2S), 2.81 (t, *J* = 7.2 Hz, 2H, CH_2CN), 1.87-1.78 (m, 12H, 6xCH_2), 1.57-1.41 [m, 36H, 6x$(CH_3)_2C$], 0.90-0.80 [m, 54H, 6x$(CH_3)_3C$], -1.94 (s, 2H, H_2Pc). IR (KBr): ν= 3098, 3027, 2954, 2918, 2849, 2232 (CN), 1585, 1504, 1464, 1392, 1364, 1273, 1216, 1173, 1074, 1014, 880 cm^{-1}. UV-Vis (THF): λ_{max}

(log ε)= 339 (4.82), 608 (4.33), 669 (4.97), 699 (4.98). HRMS (MALDI-TOF-MS) *m/z*: [M^+-H] calcd for $C_{119}H_{141}N_9O_6S$, 1823.064; found, 1823.014.

Synthesis of 2,3,9,10,16,17-hexakis-4-(*tert*-octyl)phenoxy-23-(2-cyanoethyl)thiophthalocyaninate zinc (II) (NCC_2H_4SZnPc **1**): 40 mg (0.021 mmol) of $CNC_2H_4SH_2Pc$ **4** and 14.14 mg (0.066 mmol) of $Zn(OAc)_2$ were dissolved in 3 ml of a mixture DMF:*o*-DCB/2:1 and heated up to 100°C under argon during 24 h. The crude reaction was cooled to room temperature, precipitate with methanol and purified by column chromatography using Tol:MeOH/99.5:0.5, yielding 30 mg (75%) of NCC_2H_4SZnPc (**3**). ^{1}H-NMR (300 MHz, THF-d_8, δ): 9.41 (s, 1H, ArH), 9.29 (d, *J*= 8 Hz, 1H, ArH), 8.9-8.78 (m, 5H, ArH), 8.21 (d, *J*= 8 Hz, 1H, ArH), 7.86-7.79 (m, 1H, ArH), 7.69-7.47 (m, 12H, ArH), 7.27-7.13 (m, 12H, ArH), 3.5 (XX 2H, CH_2S), 3.03 (s, 2H, CH_2CN), 1.87-1.78 (m, 12H, $6xCH_2$), 1.42-1.29 [m, 36H, $6x(CH_3)_2C$], 0.90-0.80 [m, 54H, $6x(CH_3)_3C$]. IR (KBr): ν= 3098, 3027, 2953, 2232 (CN), 1727, 1602, 1585, 1506, 1487, 1450, 1403, 1271, 1218, 1174, 1091, 1029, 893 cm^{-1}. UV-Vis (THF): λ_{max} (log ε)= 361 (4.81), 610 (4.41), 682 (5.14). HRMS (MALDI-TOF-MS) *m/z*: $[M]^+$ calcd for $C_{119}H_{139}N_9O_6SZn$, 1885.985; found, 1886.056.

Synthesis of 23-[4-(acetylthio)phenylethynyl]-2,9,16-tri-tert-butylphthalocyaninate zinc (II) ($AcSPhC_2ZnPc$ **2**): 51 mg (0.058 mmol) of iodotri-*tert*-butylphthalocyaninate zinc (II),[20] 7.2 mg (0.01 mmol) of $(Ph_3P)_2PdCl_2$ and 3.9 mg (0.02 mmol) of CuI were dissolved in 5 ml of dry THF and 4 ml of degassed DIEA. A stream of argon was passed through the solution for 10 min, then 16 mg (0.09 mmol) of 4-ethynyl-1-thioacetylbenzene[21] were added and the mixture was stirred for 15 h at rt. Solvents were removed and the resulting crude was purified by preparative TLC with $CHCl_3$:THF/100:1, obtaining 22 mg (41%) of $AcSPhC_2ZnPc$ (**4**). ^{1}H-NMR (300 MHz, DMSO-*d*$_6$, δ): 9.46-9.14 (m, 8H, ArH), 8.37-8.31 (m, 4H, ArH), 7.95-7.91 (m, 2H, ArH), 7.64 (br d, *J*= 8.2 Hz, 2H, ArH), 2.53 (br s, 3H, CH_3CO), 1.83-1.78 [m, 27H, 3x$(CH_3)_3C$]. IR (KBr): ν= 3090, 2954, 2865, 1728, 1612, 1490, 1393, 1330, 1256, 1150, 1088, 828 and 747 cm^{-1}. UV-Vis (THF): λ_{max} (log ε)= 351 (4.99), 609 (4.55), 671 (5.23) and 686 (5.26). HRMS (MALDI-TOF-MS): $[M]^+$ calcd for $C_{54}H_{46}N_8OSZn$, 918.280; found, 918.242.

Supporting Information.

Supporting Information is available from the Wiley Online Library or from the author.

Acknowledgements

This work has been supported by the Ministerio de Economía y Competividad, Generalitat Valenciana, Universitat Jaume I and the European FEDER funds (CTQ2011-26455, PROMETEO 2012/010, ACOMP/2013/024, ISIC/2012/008 and UJI 12I361.01/1).

Received: ((will be filled in by the editorial staff))
Revised: ((will be filled in by the editorial staff))
Published online: ((will be filled in by the editorial staff))

[1] O. E. Semonin, J. M. Luther, M. C. Beard, *Mater. Today.* **2012**, *15*, 508.

[2] a) V. L. Yu, H. Qu, W. Z. X. G. Guo, Peng, *Chem. Mater.* **2003**, *15*, 2854; b) C. B. Murray, D. J. Norris, M. G. Bawendi, *J. Am. Chem. Soc.* **1993**, *115*, 8706; c) K. Tvrdya, P. A. Frantsuzovc, P. V. Kamat, *PNAS* **2011**, *108*, 29.

[3] a) J. M. Luther, J. Gao, M. T. Lloyd, O. E. Semonin, M. C. Beard, A. J. Nozik, *Adv. Mater.* **2010**, *22*, 3704; b) J. Gao, C. L. Perkins, J. M. Luther, M. C. Hanna, H. –Y. Chen, O. E. Semonin, A. J. Norik, R. J. Ellingson, M. C. Beard, *Nano Lett.* **2011**,*11*, 3263.

[4] C.-H. M. Chuang, P. R. Brown, V. Bulović, M. G. Bawendi, *Nat. Mater.* **2014**, *13*, 796. http://www.nrel.gov/ncpv/images/efficiency_chart.jpg (accessed September 2014).

[5] a) L. Martín-Gomis, F. Fernández-Lázaro, Á. Sastre-Santos, *J. Mater. Chem. A*, **2014**, *2*, 15672; b) M. E. Ragoussi, M. Ince, T. Torres, *Eur. J. Org. Chem.* **2013**, 6475.

[6] a) T. Ikeuchi, H. Nomoto, N. Masaki, M. J. Griffith, S. Mori, M. Kimura, *Chem. Commun.* **2014**, *50*, 1941; b) M. -E. Ragoussi, J.-H. Yum, A. K. Chandiran, M. Ince, G. de la Torre, M. Grätzel, M. K. Nazeeruddin, T. Torres, *ChemPhysChem.* **2014**, *15*, 1033.

[7] A. Yella, C. -L. Mai, S. M. Zakeeruddin, S.-N. Chang, C.-H. Hsieh, C.-Y. Yeh, M. Grätzel, *Angew. Chem., Int. Ed.* **2014**, *53*, 2973.

[8] S. Dayal, J. Li, Y. S. Li, H. Wu, A. C. S. Samia, M. E. Kenney, C. Burda, *J. Photochem. Photobiol. A.* **2007**, *84*, 243.

[9] J. Britton, E. Antunes, T. Nyokong, *Inorg. Chem. Commun.* **2009**, *12*, 828.

[10] W. Chidawanyika, C. Litwinski, E. Antunes, T. Nyokong, *J. Photochem. Photobiol. A.* **2010**, *212*, 27.

[11] H. Lee, H. C. Leventis, S. -J. Moon, P. Chen, S. Ito, S. A. Haque, T. Torres, F. Nüesch, T. Geiger, S. M. Zakeeruddin, M. Grätzel, M. K. Nazeeruddin, *Adv. Funct. Mater.*,**2009**, *19*, 2735.

[12] V. M. Blas-Ferrando, J. Ortiz, V. González-Pedro, R. S. Sánchez, I. Mora-Seró, F. Fernández-Lázaro, Á. Sastre-Santos, *Chem. Commun.* **2015**. *51*, 1732..

[13] A. B. Sorokin, *Chem. Rev.* **2013**, *113*, 8152.

[14] F. J. Céspedes-Guirao, K. Ohkubo, S. Fukuzumi, F. Fernández-Lázaro, Á. Sastre-Santos, *Chem. Asian J.* **2011**, *6*, 3110.

[15] E. M. Maya, P. Vazquez, T. Torres, *Chem. Eur. J.* **1999**, *5*, 2004.

[16] D. T. Gryko, C. Clausen, K. M. Roth, N. Dontha, D. F. Bocian, W. G. Kuhr, J. S. Lindsey, *J. Org. Chem.* **2000**, *65*, 7345.

[17] M. S. de la Fuente, R. S. Sánchez, V. González-Pedro, P. P. Boix, S. G. Mhaisalkar, M. E. Rincón, J. Bisquert, I. Mora-Seró, *J. Chem. Phys. Lett.* **2013**, *4*, 1519.

[18] V. González-Pedro, X. Xu, I. Mora-Seró, J. Bisquert, *ACS Nano*, **2010**, *4*, 5783.

[19] F. Fabregat-Santiago, G. García-Belmonte, I. Mora-Seró, J. Bisquert, *Phys. Chem. Chem. Phys.* **2011**, *13*, 9083.

[20] a) H. Ali, J. E. van Lier, *Tetrahedron Lett.,* **1997**, 38, 1157; b) E. M. Maya, P. Vazquez, T. Torres, *Chem. Commun.,* **1997**, 1175.

[21] D. T. Gryko, C. Clausen, K. M. Roth, N. Dontha, D. F. Bocian, W. G. Kuhr, J. S. Lindsey, *J. Org. Chem.* **2000,** *65,* 7345.

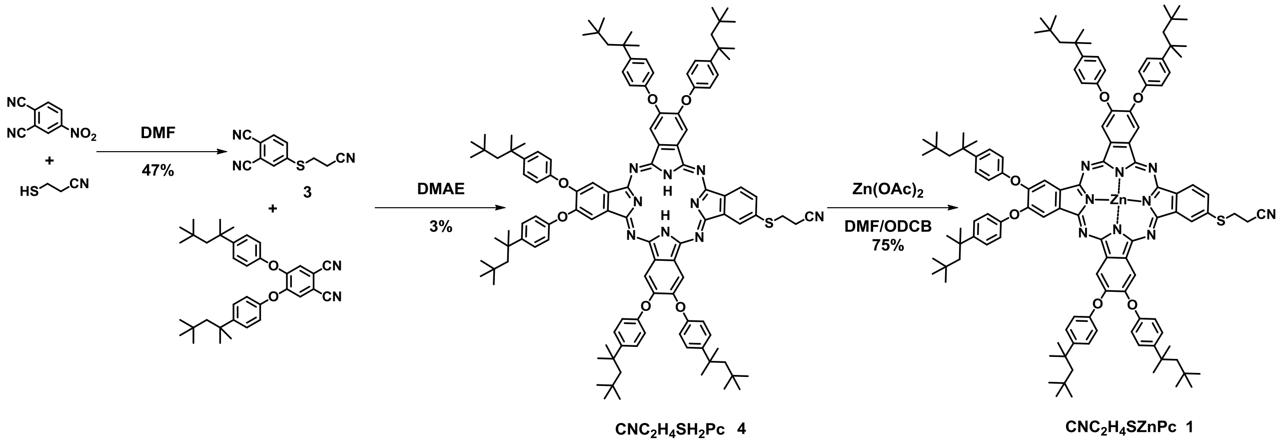
NC
NC
NO2
+
HS
CN
DMF
47%
NC
NC
S
CN
3
+
O
O
CN
CN
DMAE
3%
N
H
S
CN
Zn(OAc)2
DMF/ODCB
75%
Zn
CNC2H4SH2Pc 4
CNC2H4SZnPc 1

Scheme 1.

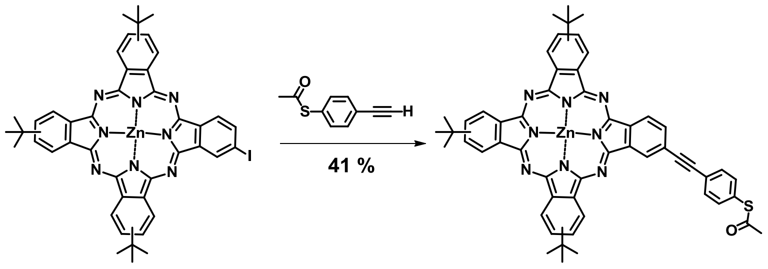

AcSPhC$_2$ZnPc **2**

Scheme 2.

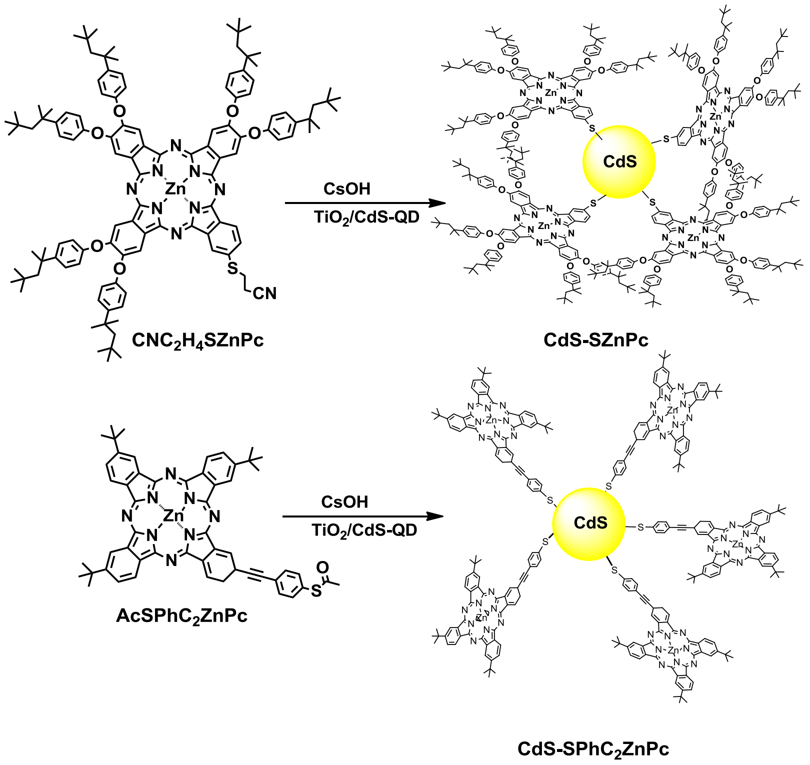
CsOH
TiO_2/CdS-QD
CNC$_2$H$_4$SZnPc
CdS-SZnPc
CdS
CsOH
TiO_2/CdS-QD
AcSPhC$_2$ZnPc
CdS-SPhC$_2$ZnPc
CdS

Scheme 3.

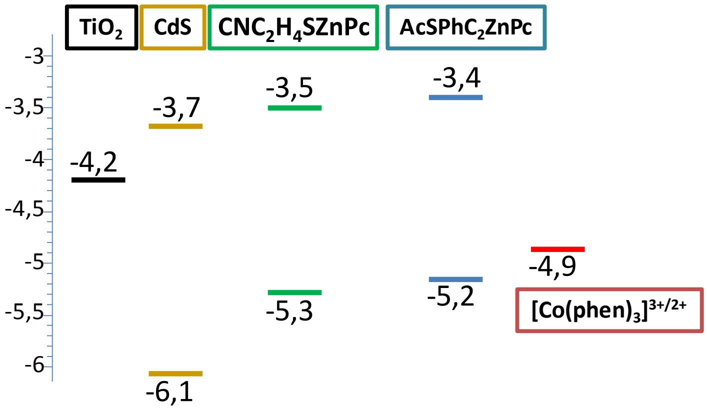
TiO$_2$
CdS
CNC$_2$H$_4$SZnPc
AcSPhC$_2$ZnPc
-3
-3,5
-4
-4,5
-5
-5,5
-6
-4,2
-3,7
-6,1
-3,5
-5,3
-3,4
-5,2
-4,9
[Co(phen)$_3$]$^{3+/2+}$

Figure 1

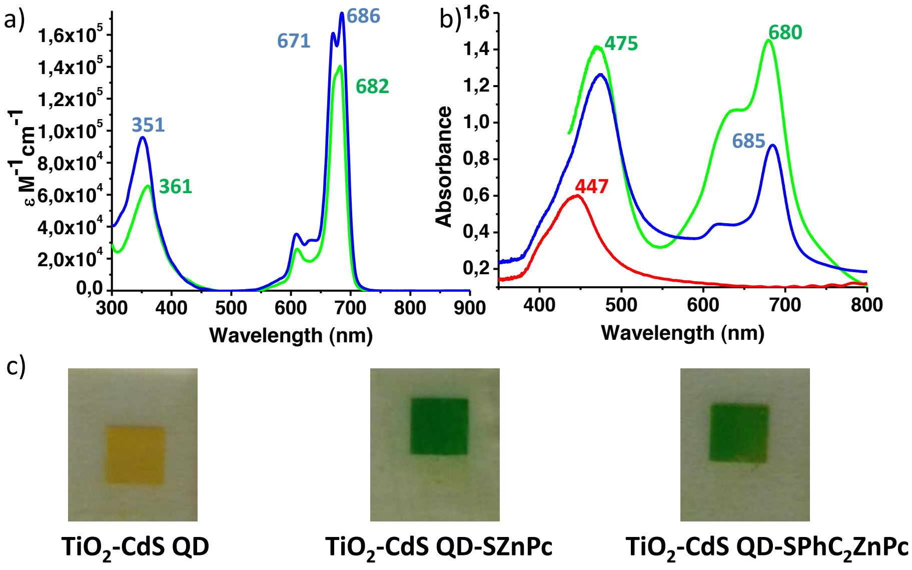
a)
b)
c)
ε M^{-1}cm^{-1}
0,0
2,0x10^4
4,0x10^4
6,0x10^4
8,0x10^4
1,0x10^5
1,2x10^5
1,4x10^5
1,6x10^5
351
361
671
686
682
300
400
500
600
700
800
900
Wavelength (nm)
Absorbance
0,2
0,4
0,6
0,8
1,0
1,2
1,4
1,6
475
680
685
447
400
500
600
700
800
Wavelength (nm)
TiO$_2$-CdS QD
TiO$_2$-CdS QD-SZnPc
TiO$_2$-CdS QD-SPhC$_2$ZnPc

Figure 2

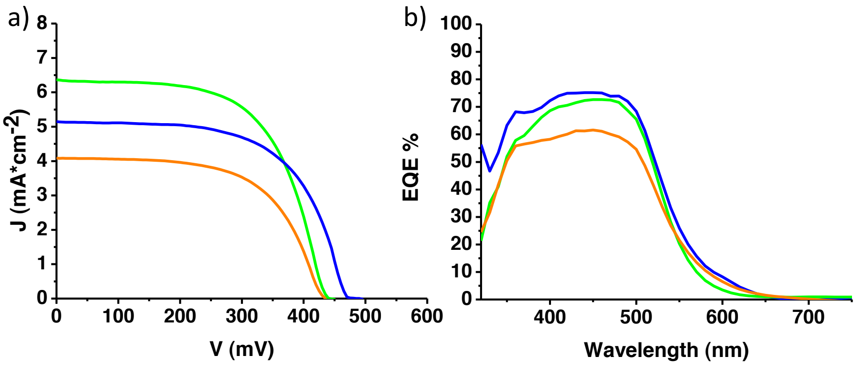
a)
J (mA*cm^{-2})
0
1
2
3
4
5
6
7
8
V (mV)
0
100
200
300
400
500
600
b)
EQE %
0
10
20
30
40
50
60
70
80
90
100
Wavelength (nm)
400
500
600
700

Figure 3

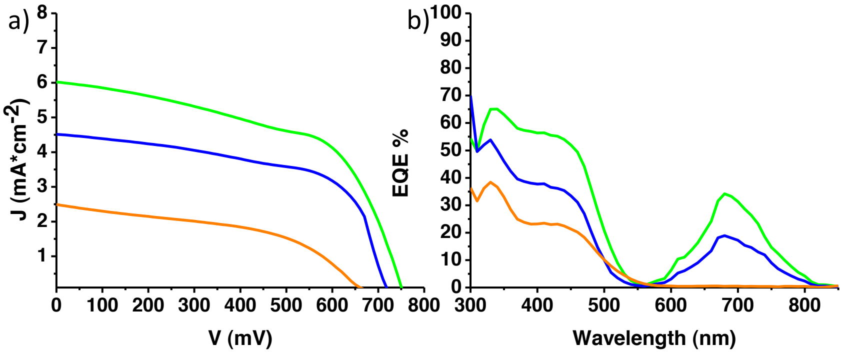
a)
J (mA*cm^{-2})
8
7
6
5
4
3
2
1
0
100
200
300
400
500
600
700
800
V (mV)
b)
EQE %
100
90
80
70
60
50
40
30
20
10
0
300
400
500
600
700
800
Wavelength (nm)

Figure 4

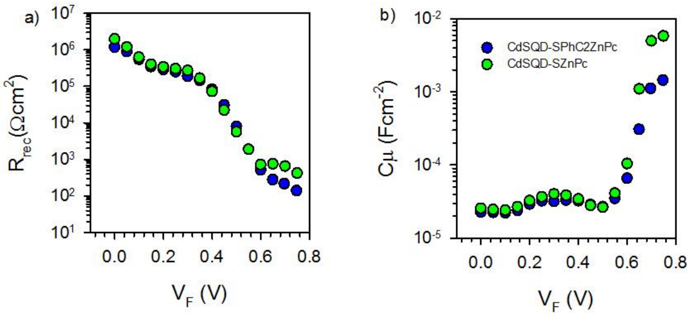
a)
$R_{rec}(\Omega cm^2)$
10^7
10^6
10^5
10^4
10^3
10^2
10^1
0.0
0.2
0.4
0.6
0.8
V_F (V)
b)
$C\mu$ (Fcm^{-2})
10^{-2}
10^{-3}
10^{-4}
10^{-5}
CdSQD-SPhC2ZnPc
CdSQD-SZnPc
0.0
0.2
0.4
0.6
0.8
V_F (V)

Figure 5

QD-ZnPc	***Electrolyte***	***t***	***Jsc***	***Voc***	***FF***	η	***EQE***
		h	***[mA*cm^{-2}]***	***[mV]***		***%***	***%***
CdS	S^{2-}/S_n^{2-}	-	4.08	437	59.5	1.1	57$^{a)}$
CdS/THF	S^{2-}/S_n^{2-}	4	5.51	412	56	1.2	
CdS-NCC$_2$H$_4$SZnPc	S^{2-}/S_n^{2-}	4	6.35	441	60.1	1.7	72^a
CdS-AcSPhC$_2$ZnPc	S^{2-}/S_n^{2-}	4	5.14	479	60	1.5	75^a
CdS	[Co(phen)$_3$]$^{3+}$/$^{2+}$	-	2.49	654	42.2	0.8	25^a
CdS-NCC$_2$H$_4$SZnPc	[Co(phen)$_3$]$^{3+}$/$^{2+}$	4	6.02	750	55.2	2.5	58^a, 35^b
CdS-AcSPhC$_2$ZnPc	[Co(phen)$_3$]$^{3+}$/$^{2+}$	4	4.52	734	58	1.9	39^a, 20^b

a) λ_{max} = 420 nm; b) λ_{max} = 685nm.

Table 1

Figure Captions

Scheme 1. Synthesis of CNC_2H_4SZnPc 1

Scheme 2. Synthesis of $AcSPhC_2ZnPc$ 2.

Scheme 3. Preparation of CdS-SZnPc and CdS-$SPhC_2ZnPc$ hybrid systems.

Figure 1. Energy levels of TiO_2, CdS, CNC_2H_4SZnPc and $AcSPhC_2ZnPc$ and $[Co(phen)_3]^{3+}/^{2+}$.

Figure 2. (a) Absorbance measurements in THF as solvent of CNC_2H_4SZnPc (green line) and $AcSPhC_2ZnPc$ (blue line) (b) Absorbance measurements of the QDSC devices: QD CdS (red line), CdS QD-SZnPc (green line) and CdS QD-$SPhC_2ZnPc$ (blue line). (c) Absorbance measurements of the QDSC devices: TiO_2-CdS QD, TiO_2-CdS QD-SZnPc and TiO_2-CdS QD-$SPhC_2ZnPc$ (reference absorption of TiO_2 substracted has been substracted).

Figure 3. (a) *J-V* curve and (b) EQE curve of QDSC devices using electrolyte with S^{2-}/S_n^{2-} redox: CdS ref (orange line), CdS QD-SZnPc (green line) and CdS QD-$SPhC_2ZnPc$ (blue line).

Figure 4. (a) *J-V* curve and (b) IPCE curve of QDSC devices using electrolyte with $[Co(phen)_3]^{3+}/[Co(phen)_3]^{2+}$ redox: CdS ref (orange line), CdS QD-SZnPc (green line) and CdS QD-$SPhC_2ZnPc$ (blue line).

Figure 5. Impedance spectroscopy analysis. a) Recombination resistance, R_{rec}, and b) Chemical capacitance, C_{μ}, as a function of voltage, V_F (removing the effect of series resistance).

Table 1. Values obtained from the QDSC devices with the following architecture: FTO/TiO_2/ QDs/ Electrolyte.